






Dipole alignment of water molecules flowing through a carbon nanotubeHemant Kumar ^{1,*}, Saheb Bera ¹, Subhadeep Dasgupta ², A. K. Sood,² Chandan Dasgupta ^{2,3} and Prabal K. Maiti ^{2,†}¹*School of Basic Sciences, Indian Institute of Technology Bhubaneswar, Argul, Odisha 752050, India*²*Department of Physics, Indian Institute of Science, Bangalore 560012, India*³*International Centre for Theoretical Sciences, TIFR, Bangalore 560089, India*

(Received 17 September 2021; revised 2 March 2023; accepted 14 March 2023; published 3 April 2023)

The flow of water through nanochannels has promising applications in desalination, energy conversion, and nanomedicine. We have used molecular dynamics simulations to show that the water molecules passing through a wide single-walled carbon nanotube (CNT) get aligned by the flow to have a net dipole moment along the flow direction. With increasing flow velocity, the net dipole moment first increases and eventually saturates to a constant value. This behavior is similar to that of an Ising chain with the flow velocity acting as an effective aligning field. We show that the microscopic origin of this behavior is the preferential entry of water molecules with their dipole vectors pointing inward along the CNT axis.

DOI: [10.1103/PhysRevB.107.165402](https://doi.org/10.1103/PhysRevB.107.165402)**I. INTRODUCTION**

Recent years have seen an upsurge of interest in exploring ultrafast transport of water in various nanochannels with potential applications such as desalination, separation processes, and energy conversion [1–11]. However, a quantitative understanding of flow-induced effects in nanochannels is still lacking [12,13]. Recent progress in nanofabrication and the development of measurement techniques have enabled direct investigation of fluids confined in nanochannels [14–18]. Tunuguntla *et al.* demonstrated a high permeability of water across narrow carbon nanotubes of diameter ~ 0.8 nm and significantly lower permeability for wider CNTs (diameter ~ 1.5 nm) [19]. Radha *et al.* observed relatively fast flow rates when a slit pore is narrow to accommodate only a monolayer of water molecules [20].

However, a clear association of structural changes with flow rate has not been demonstrated yet [21]. Yuan *et al.* have shown, using *ab initio* molecular simulation, that the net dipole moment of water molecules inside a carbon nanotube can polarize the tube, thus creating a potential difference between the nanotube ends [22]. Ghosh *et al.* have shown experimentally the generation of voltage (and current) across CNTs due to pressure-induced flow of water molecules across nanotube bundles [23]. This observation motivated us to ask if water dipoles order when water flows inside a CNT. The answer indeed is in the affirmative as shown in our present molecular dynamics (MD) simulations.

Water molecules in equilibrium inside narrow carbon nanotubes (diameter ~ 0.8 nm) are arranged in a single-file manner, with the projections of all the dipoles along the nanotube axis pointing in the same directions [24,25]. These dipoles flip collectively on a time scale that increases with the length of the nanotube [26]. Lin *et al.* have shown that in equilibrium, the dielectric relaxation of confined water

molecules inside CNTs is much faster along the cross section than along the axis [27]. However, as the diameter of the nanotube increases, water molecules are no longer arranged in a single-file manner, and there is no apparent ordering at ambient conditions of pressure and temperature.

In this paper, we demonstrate that the water dipoles confined inside a wider (10, 10) nanotube (diameter 1.4 nm), which exhibits no net dipole polarization in equilibrium, can show net dipole ordering under the effect of flow generated by a pressure gradient. The alignment of the net dipole moment along the flow direction increases with flow velocity, eventually saturating at a finite value. This behavior of confined water can be very well explained by treating them as Ising spinlike dipoles under effective aligning fields at the boundaries that depend on the flow velocity. The effective fields arise from the asymmetric dielectric interfaces at the CNT ends where water molecules from the bulk enter the CNT cavity. This observation not only demonstrates the existence of a novel physical phenomenon but also suggests pathways for various nanoelectromechanical devices.

II. METHOD AND SIMULATION DETAILS

We have performed MD simulations of a 10 nm long arm-chair (10, 10) carbon nanotube (diameter 1.4 nm) solvated in TIP3P [28] water as shown in Fig. 1(a) using LAMMPS [29]. Carbon atoms were modeled as uncharged Lennard-Jones (LJ) particles with parameters taken from AMBER force field [30,31]. Interaction between water and carbon atoms was included through LJ interaction between carbon and oxygen atoms. Long-range electrostatic interactions between charged entities were computed using PPPM algorithm with a real space cutoff of 10 Å [29]. We initially run an equilibrium MD simulation in NPT keeping the temperature at 280 K and pressure at 1 atm. Nosé-Hoover thermostat and barostat as implemented in LAMMPS were used to maintain the constant temperature and pressure [32,33]. After equilibrating the system at $T = 280$ K and $P = 1$ atm, we switched to NVT ensemble using Nosé-Hoover thermostat with a coupling

*hemant@iitbbs.ac.in

†maiti@iisc.ac.in

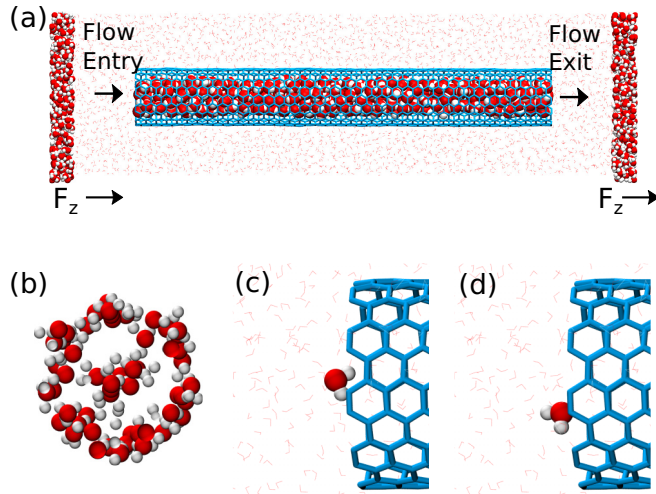


FIG. 1. (a) Simulated system, highlighted water molecules at both ends represent the layers on which additional force was applied to simulate the flow. (b) Structure of water molecules confined inside the carbon nanotube. A typical water molecule before entering the CNT with dipole pointing inward (c) and outward (d).

constant of 1 ps. To simulate pressure gradient-induced flow, we pushed a 5 Å layer of water at both ends of the water box along the nanotube axis by adding extra force on the oxygen atoms of each water molecule lying in these layers [Fig. 1(a)]. This protocol for simulating hydrostatic pressure gradients is known to mimic pressure-induced flow [34]. We waited for 5 ns of simulation time to achieve a steady state. Later, 50 ns of flow simulation was used to analyze the behavior of water dipoles at different flow velocities.

III. RESULTS

A. Flow-dependent arrangement of confined water molecules

At equilibrium, when there is no flow, water molecules confined in the CNT spend an almost equal amount of time in

orientations for which the projections of their dipole moments ($\vec{\mu}_w$) along the nanotube axis (\hat{z} axis) are positive and negative, and the average dipole moment of the confined water molecules over a long trajectory is zero. Figure 2(a) shows the probability of finding a molecular dipole in a particular alignment [$\theta_w = \cos^{-1}(\hat{z} \cdot \vec{\mu}_w)$] for different flow velocities. Equal height peaks at $\theta_w = 36^\circ$ and $\theta_w = 144^\circ$ in equilibrium demonstrate equal preference for both alignments. At finite flow velocity, more dipoles prefer to be aligned along the flow direction. Figure 2(a) clearly brings out that the probability of alignment along the flow direction ($+\hat{z}$ direction) at $\theta_w = 36^\circ$ increases while the probability of alignment opposite to the flow direction (peak at $\theta_w = 144^\circ$) ($-\hat{z}$ direction) decreases, leading to a net dipole moment along the direction of flow. To investigate the nature of this alignment, we study the spatial ordering of confined water molecules for different flow velocities by calculating the pair-correlation function $g(z)$ of the confined water molecule using $g(z) = \frac{1}{N} \sum_{i=1}^N \sum_{j>i}^N \frac{\delta(z-z_{ij})}{N}$, where N is the number of water molecules inside the nanotube in each snapshot of the system and z_{ij} is the separation along the nanotube axis between i^{th} and j^{th} water molecules. The computed pair correlation functions for the confined water molecules at different flow velocities demonstrate that $g(z)$ is almost independent of flow velocity with a very slight increase in the ordering at higher flow velocities (Fig. S1) [35]. This implies that the flow does not alter positional ordering, but its net effect is to create an aligning field that tends to orient the dipoles of confined water molecules in the direction of flow.

B. Flow-induced alignment of confined water molecules

The temporal evolution of the net dipole projection $D(t) = [\sum_w \cos \theta_w(t)]/N$ of all confined water molecules shown in the inset of Fig. 2(b) indicates that the confined molecules prefer two states with the projections of their dipole moments along the CNT axis collectively pointing in the $+\hat{z}$ and $-\hat{z}$ directions. A flip between parallel (along the flow) and antiparallel (opposite to the flow) aligned states occurs at regular time intervals. (Data shown here is for a 10 nm long CNT,

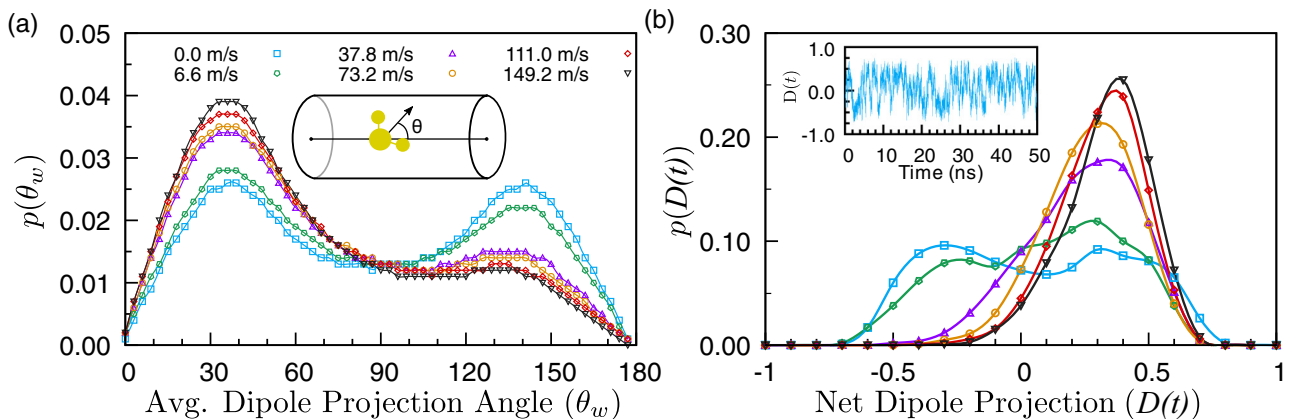


FIG. 2. (a) Distribution of the angle θ_w between the dipole moment of individual water molecules inside a (10, 10) carbon nanotube and the flow direction. In the absence of flow, the probability shows peaks of equal height at $\theta_w = 36^\circ$ and $\theta_w = 144^\circ$. Flow creates asymmetry, and more dipoles are orientated along the flow direction. (b) Probability distribution of the net dipole projection $D(t)$ of all confined water molecules for various flow velocities. Inset shows the temporal variation of the net dipole projection of confined water molecules along the CNT axis in equilibrium.

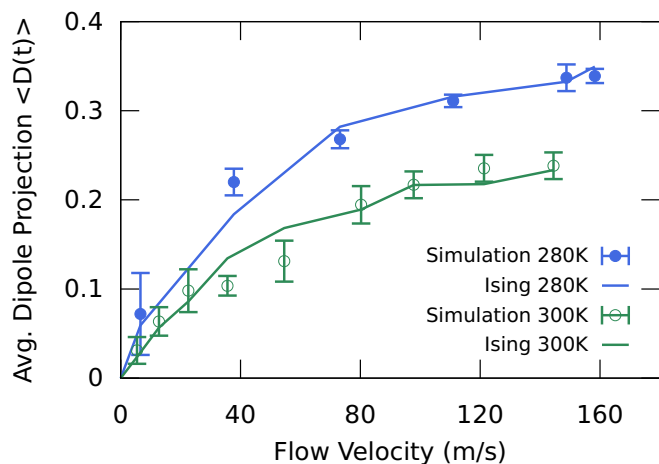


FIG. 3. Variation of the average dipole moment per molecule of the confined water molecules, projected in the flow direction, with the flow velocity for temperatures $T = 280$ K and 300 K. The variation can be fitted well with the results for a 1D Ising model with flow-dependent fields [Eq. (1): $\beta\mu_w[e_L(v) - e_R] = 0.01264 v$ for $T = 280$ K]. The same velocity and field relation with appropriate temperature scaling (with 5% higher equilibrium fields) also reproduce the alignment behavior at $T = 300$ K, which implies that the flow effect can be well described by an effective field created due to the flowing water molecules.

as the length of the CNT increases, this description becomes more accurate, as shown in Fig. S2) [35]. The probability distribution of the net dipole projection $D(t)$ shown in Fig. 2(b) depicts that the probabilities of finding a net dipole projection

along $+\hat{z}$ and $-\hat{z}$ directions are almost equal without flow, and hence, the average dipole projection is zero. As the flow velocity increases, the probability of finding a net dipole projection aligned with the flow direction increases, as is evident from the increasing height of the peak near the net dipole projection of 0.4 and decreasing height of the peak around -0.4 that corresponds to the antiparallel aligned state. Figure 3 shows the variation of the average projection $D = \langle D(t) \rangle$ of the net dipole moment vector of the confined water molecules. At a given temperature ($T = 280$ K), increasing the flow velocity increases the average dipole projection (D) in the flow direction, and then it saturates to a constant value of ~ 0.34 . This value is less than 1 because perfect alignment along the axis is energetically unfavorable due to the loss of hydrogen bonds as well as likely to be entropically unfavorable due to enhanced order.

To understand this flow-induced alignment, we compute the average duration for which the confined molecules continuously remain aligned before initiating a successful orientational flip to the opposite alignment. We start by simplifying the dipole projection trajectory by allowing only three possible values for the projection such that a state corresponding to net projection ≥ 0.1 is assigned a projection of 1 (parallel to the flow), ≤ -0.1 is assigned as -1 (antiparallel to flow), and anything between 0.1 to -0.1 is assigned as 0 (transition state). The variation of the average dwell time of parallel and antiparallel alignments with the flow velocity extracted from this modified trajectory is shown in Fig. 4(a). It clearly demonstrates that the average dwell time for the parallel aligned state increases and that for the antiparallel state decreases with increasing flow velocity.

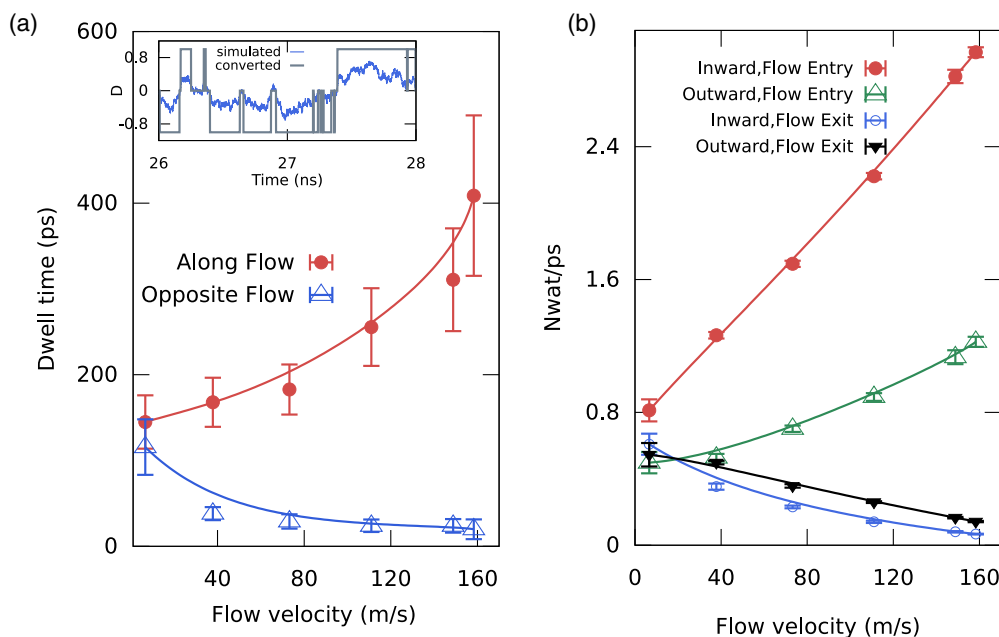


FIG. 4. (a) The variation of the average dwell time for both alignment states with the flow velocity. The dwell time increases with the flow velocity for the parallel alignment and decreases for the state of antiparallel alignment. The inset shows the construction of the simplified dipole projection trajectory described in the text. (b) The number of water molecules entering from the bulk into the CNT cavity with their dipole moments pointing inward or outward. More water molecules enter with dipole pointing inward to the nanotube from both ends at equilibrium. As the flow velocity increases from zero, the flux from the flow-entry end increases while the flux from the opposite end decreases. (Lines are guides to the eye only).

C. Reorientation of confined water under flow

In order to get insights into how flow impacts the dwell time, we analyze the reorientation mechanism of water molecules in equilibrium conditions [36,37]. Dipole reorientation inside narrow CNTs, where the dipoles are aligned in a single file manner, is initiated through defect nucleation at one of the CNT ends [26]. When a water molecule enters the CNT such that its dipole is pointing in the opposite direction to those of the confined water dipoles, it is characterized as an orientational defect. When such a defect moves through the confined water chain, it leaves behind flipped individual dipoles. A successful collective flip of the dipole moments occurs when a defect entering from one end exits from the other end. A similar reorientation mechanism can be extended for the wider CNT considered here (Fig. S3 [35]).

D. Preferred entry of inward-pointing dipole

We characterize the dipole moments of water molecules that enter the CNT from the two ends, and then, separated the entry events based on the dipole moment of the entering water molecules. A strong preference was observed for water molecules to enter with dipoles pointing inward (dipole projection >0 for the left end, <0 for the right end) in the equilibrium condition. Of all the water molecules entering inside the CNT cavity from both ends, 55.5% of water molecules have dipole pointing inward while only 44.5% have dipole pointing outward. We also found that the average interaction energy of a water molecule just before entry with its dipole vector pointing inward is -9.798 kcal/mol and -9.391 kcal/mol for the outward-pointing dipole vector of the entering water molecule. This preference arises due to distinct hydrogen bonding environments near the entrance of the nanotube for the two dipole orientations, as highlighted in Figs. 1(c) and 1(d). Due to different surrounding environments, the average number of hydrogen bonds for an inward-pointing dipole is 3.8 as compared to 3.4 for the outward-pointing dipoles, thus showing energetics to be responsible for the preferred entry of molecules with inward-pointing dipoles.

E. Mechanism of flow-induced alignment of water molecules

Favorable bias for the entry of inward-pointing water molecules and defect-assisted orientational flip mechanism are the key ingredients to understand the emergence of net alignment due to flow. In the absence of flow, the influx is the same for both ends of the CNT. Hence the probability of defect nucleation to initiate a collective dipole flip is the same for both net alignments. This explains the similar dwell times for both alignments. However, during the flow, a larger number of water molecules enter from the flow-entry edge of CNT as compared to the flow-exit edge. As there is a strong preference for water molecules to enter with their dipoles pointing inward, more water molecules will enter through the flow-entry end with dipole pointing in the flow direction [Fig. 4(b)]. These water molecules do not destroy the alignment of the dipoles inside the CNT if the alignment is in the flow direction. The situation is reversed if the alignment of the dipoles inside the CNT is opposite to the flow direction: in that case, the larger number of water molecules entering with dipole

moments pointing inward act as defects that can lead to a collective flip of the dipolar alignment. Hence, the probability of a reorientational flip is higher for antiparallel alignment. The net effect of preferred orientation at the flow-entry edge is to increase the probability of defect nucleation for antiparallel alignment. At the opposite end, water molecules prefer to enter with their dipoles pointing opposite to the flow (inward). Such entry events are likely to initiate flips for a parallel aligned state. However, being the flow-exit edge, the influx from this end decreases with the flow velocity resulting in a reduced probability of flipping for the parallel aligned state [Fig. 4(b)].

F. Equivalent Ising-like model

To validate if such preferred entry of inward-pointing dipole can explain the emergence of flow-induced alignment, we propose a one-dimensional (1D) Ising-like model for confined water molecules. Bistable orientation of confined water molecules is modeled by assigning Ising spinlike behavior to the water dipoles of moment $\vec{\mu}_w$ where $|\vec{\mu}_w| = 2.3$ Debye. Dipole-dipole interaction is included as a ferromagnetic exchange interaction between nearest neighbors. The preferred entry of inward-pointing dipoles is modeled through aligning fields e_L and e_R at the left and right ends of the CNT, respectively. The effective Hamiltonian can be written as:

$$H = -J \sum_{i<N} \mu_i \cdot \mu_{i+1} - e_L \mu_1 + e_R \mu_N \quad (1)$$

with $e_L, e_R > 0$. In the absence of flow, e_L and e_R are equal and the effect of the flow is incorporated by considering e_L to be a flow-dependent quantity. We simulate this model with $N = 250$ dipoles using the Metropolis algorithm at temperature $\beta J = 7.64$, which is equated to the dipole-dipole interaction between water dipoles at $T = 280K$. In the absence of flow ($e_L = e_R$), the dipole configuration fluctuates between equally probable left- and right-aligned states (positive and negative magnetization states of the Ising model) and the net dipole projection is 0, as shown in Fig. 5(a). The average net dipole moment increases with increasing the field e_L as shown in Fig. 5(a). This behavior is very similar to the flow-induced alignment observed in our MD simulations (Fig. 3). This motivated us to compute an aligning field for each flow velocity. The aligning field can be extracted by comparing the flow-induced alignment with the field-induced alignment of the Ising spins and assigning a field to each flow velocity that matches the same alignment values. The extracted alignment fields for all flow velocities show a linear relation $\beta \mu_w [e_L(v) - e_R] = 0.01264v$, as shown in Fig. 5(b). The net dipole alignment as obtained from the proposed model simulated with the extracted field values shows excellent agreement with the MD simulations (Fig. 3) suggesting that such asymmetries at the boundaries can indeed lead to the observed effect.

G. Length dependence

Such boundary-induced effects are likely to depend on system size: the net dipole alignment may decrease with increasing length of the CNT. On the contrary, simulation for two different lengths (3 and 5 nm), suggests that the net

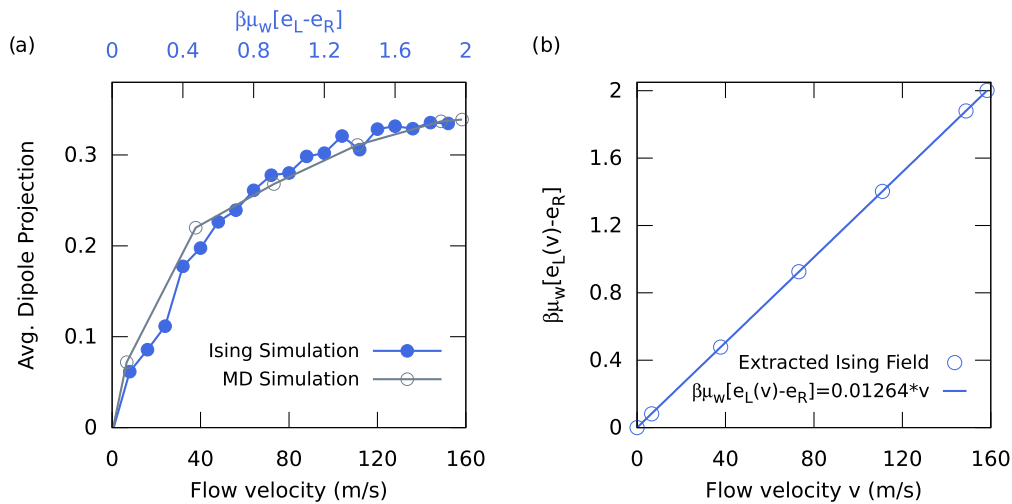


FIG. 5. The procedure to find the equivalent electric field for each flow velocity. (a) 1D Ising model was simulated for the varying amount of the field at the flow entry end. The average moment for each field is plotted and compared with the flow-induced alignment from the MD simulation. An equivalent field which causes the same average dipole projection was assigned for each flow velocity. (b) The variation of the extracted electric field with the flow velocity. A linear relationship was obtained, given by $\beta\mu_w[e_L(v) - e_R] = 0.01264v$.

alignment is higher for longer CNTs (Fig. 6), for the same flow velocity and temperature. To investigate this length dependence further, we compare the average net dipole alignment for four different CNT lengths at a high flow velocity approximately leading to the dipole moment saturation as shown in the inset of Fig. 6. These results indicate that flow-induced net alignment is observed for all lengths including the longest CNT of 20 nm length. As nonzero net alignment emerges when confined water molecules spend more time in the parallel-aligned state as compared to the antiparallel-aligned state, the length dependence of the net dipole alignment can be understood from the variation of the average dwell times for both alignment states with CNT length. To explore this, we compute the dwell time for different CNT lengths. As shown in the Fig. S4, we observe longer

dwell times for both alignments for longer CNTs [35]. The microscopic origin of this dependence can be understood from the reorientational mechanism discussed above.

The dwell time for a state depends on the probability of nucleation of an orientational defect at one end of the CNT and its propagation to the other end. Mukherjee *et al.* have shown that for narrow CNTs, the probability of a successful entry of an orientational defect decreases with increasing nanotube length as the dipole-induced electric field at the ends increases due to a larger magnitude of the net dipole moment inside a longer CNT [26]. This effect, as well as the longer time taken by a defect to traverse a longer CNT, lead to longer dwell times for both alignments in equilibrium, which we observe here for wider CNTs as well (Fig. S4 [35]). The preference of a water molecule to enter the CNT with its dipole moment pointing inward is also enhanced as the length of the CNT is increased. This enhancement is evident from the computed ratio of inward flux to outward flux, which is higher for longer CNTs (1.13, 1.25, and 2.52 for 3, 10, and 20 nm long CNTs, respectively). Based on this observation, a qualitative argument can be made to explain the length dependence of flow-induced alignment observed in our MD simulations. The higher influx of inward-pointing water molecules for longer CNTs indicates that a dipole at the flow entry end feels a higher electric field compared to shorter CNTs. This enhanced field helps to maintain dipole order for longer lengths of the CNT. It is apparent from the above discussion that the proposed mechanism is valid only when all the confined water molecules arrange themselves such that all dipoles are collectively oriented in the same direction and the net dipole alignment exhibits bistable behavior. Kofinger *et al.* have estimated that this length for narrow (6, 6) CNTs is approximately 0.1 mm [38]. To zeroth-order approximation, wider (10, 10) CNTs can be approximated to have a correlation length of the same order, indicating that such alignment effects will also be present for significantly longer CNTs than those studied here and reaffirming the possibility of observing the alignment in experiments for longer CNTs.

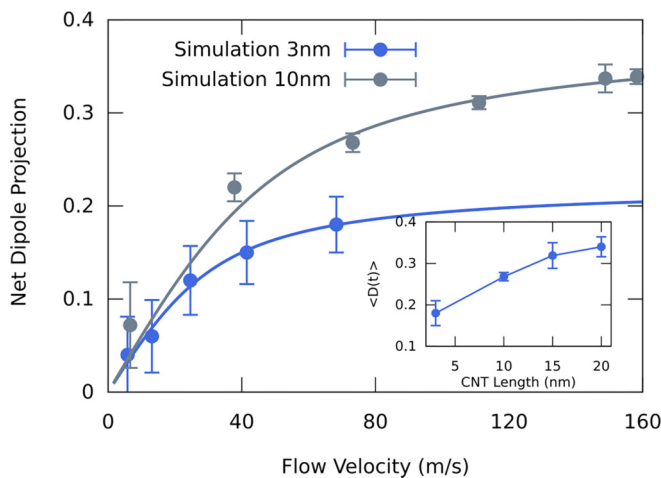


FIG. 6. Variation of the net dipole moment of the confined water molecules with flow velocity for two different lengths of CNT, 3 nm and 10 nm. The average dipole moment increases as the length of the CNT increases. (Lines are guides to the eye only). Inset shows the net alignment for different CNT lengths at $T = 280$ K with flow velocities = 60 ± 10 m/s.

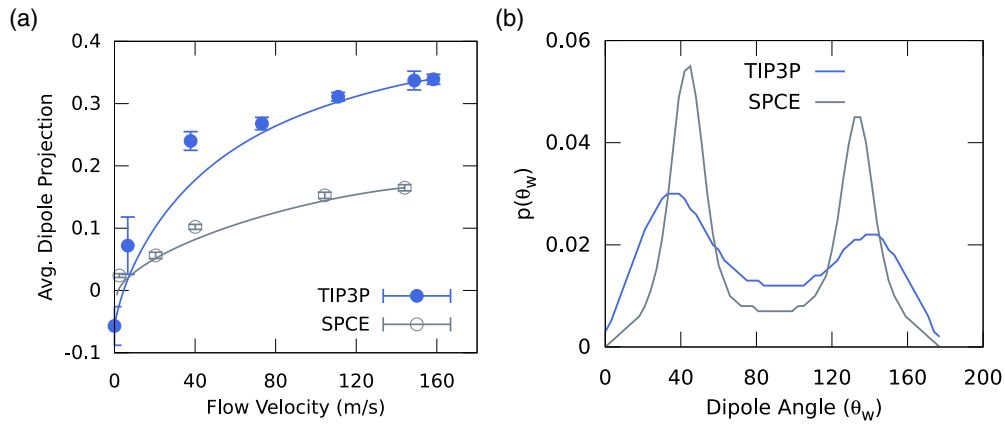


FIG. 7. Dependence of the dipole alignment on water models. (a) Variation of the average dipole projection of the water molecules confined inside 10 nm long (10, 10) CNT with flow velocity for two different water models, namely TIP3P and SPC/E. (b) The probability distribution for the angle that the dipole moment of a confined water molecule makes with the CNT axis in equilibrium conditions.

H. Force field dependence

To check if this effect is present for other water models, we repeated the study with the SPC/E water model at $T = 280$ K, and compared the results with those for the TIP3P water model. As shown in Fig. 7(a), flow-induced alignment is also observed for SPC/E water molecules for all flow velocities studied here. However, the value of the average net dipole alignment is lower for the SPC/E model than that for the TIP3P model. Owing to different interatomic potentials, the two water models exhibit slightly different molecular arrangement inside a CNT even under equilibrium conditions. The probability distribution for the angle that the dipole vector of a confined water molecules makes with the CNT axis in equilibrium, shown in Fig. 7(b), indicates that a majority of the SPC/E water molecules make an angle of 45° (135° for opposite alignment), while the probability distribution peaks at 36° (144° for opposite alignment) for the TIP3P water model. Since, on the average, SPC/E water molecules make a larger angle with the CNT axis, the net dipole projection for SPC/E is smaller (± 0.26) compared to (± 0.4) for TIP3P. The saturation value of the dipole projection for high flow velocities corresponds to the situation in which a flip from the positive dipole projection state (right) to the negative projection state (left) is extremely rare. So, the saturation value is capped at the maximum possible value of the net projection, which is lower for the SPC/E model. This explains the lower value of the saturation moment observed for the SPC/E model compared to TIP3P as a consequence of a different structural arrangement originating from different interactions.

IV. CONCLUSION

To summarize, we have demonstrated that a net dipole alignment in the flow direction emerges for water molecules flowing through a (10, 10) CNT, and the dipole alignment

increases with the flow velocity. The net alignment arises due to the asymmetry in the dipole orientation with which water molecules enter the nanotube. The preferential entry of water molecules with dipoles pointing inward decreases (increases) the probability of orientational flips when the confined water dipoles are aligned parallel (antiparallel) to the flow direction. This makes the time-averaged net dipole projection in the steady state to point in the flow direction. This observation presents a unique example where confinement produces entirely different behavior from its bulk counterparts.

The correlation between dipole alignment and flow rate can be exploited for various nanofluidic devices as it gives us a way to control the net dipole moment via external pressure. This observation also raises an important question: is dipolar alignment necessary for the ultrafast transport observed in narrow nanopores? The answer to this question requires a more detailed investigation. The net dipole moment of water inside a carbon nanotube can polarize it, and this effect can be used to engineer a potential difference across nanotube ends [22]. As demonstrated here, such polarization can be obtained inside wider nanotubes that confine more significant dipole moments per unit length. It will potentially lead to more significant potential differences across the nanotube ends. As the flow modulates dipole relaxation, this also offers a possibility of making devices in which the flow velocity of the water controls the dielectric constant.

ACKNOWLEDGMENTS

H.K. would like to thank National PARAM Supercomputing Facility at C-DAC, India and SAMKHYA: HPC Facility at IoP, Bhubaneswar. S.B. acknowledges financial support from CSIR, India. S.D., P.K.M., C.D., and A.K.S. thank DST, India for financial support.

- [1] L. Bocquet, *Nature Mater.* **19**, 254 (2020).
 [2] Q. Xie, M. A. Alibakhshi, S. Jiao, Z. Xu, M. Hempel, J. Kong, H. G. Park, and C. Duan, *Nature Nanotechnol.* **13**, 238 (2018).

- [3] J. Shen, G. Liu, Y. Han, and W. Jin, *Nat. Rev. Mater.* **6**, 294 (2021).
 [4] J. Rabinowitz, C. Cohen, and K. L. Shepard, *Nano Lett.* **20**, 1148 (2020).

- [5] B. Bao, J. Feng, J. Qiu, and S. Zhao, *ACS Omega* **6**, 943 (2021).
- [6] K. Falk, F. Sedlmeier, L. Joly, R. R. Netz, and L. Bocquet, *Nano Lett.* **10**, 4067 (2010).
- [7] A. Siria, P. Poncharal, A.-L. Biance, R. Fulcrand, X. Blase, S. T. Purcell, and L. Bocquet, *Nature (London)* **494**, 455 (2013).
- [8] M. Heiraniyan, A. Taqieddin, and N. R. Aluru, *Phys. Rev. Res.* **2**, 043153 (2020).
- [9] J. Chen, X.-Z. Li, Q. Zhang, A. Michaelides, and E. Wang, *Phys. Chem. Chem. Phys.* **15**, 6344 (2013).
- [10] S. J. Davis, M. Macha, A. Chernev, D. M. Huang, A. Radenovic, and S. Marion, *Nano Lett.* **20**, 8089 (2020).
- [11] Q.-L. Zhang, W.-Z. Jiang, J. Liu, R.-D. Miao, and N. Sheng, *Phys. Rev. Lett.* **110**, 254501 (2013).
- [12] M. Heiraniyan and N. R. Aluru, *ACS Nano* **14**, 272 (2020).
- [13] X. Gong, J. Li, H. Zhang, R. Wan, H. Lu, S. Wang, and H. Fang, *Phys. Rev. Lett.* **101**, 257801 (2008).
- [14] H. Li, J. Zhong, Y. Pang, S. H. Zandavi, A. H. Persad, Y. Xu, F. Mostowfi, and D. Sinton, *Nanoscale* **9**, 9556 (2017).
- [15] J. Zhong, M. A. Alibakhshi, Q. Xie, J. Riordon, Y. Xu, C. Duan, and D. Sinton, *Acc. Chem. Res.* **53**, 347 (2020).
- [16] K. V. Agrawal, S. Shimizu, L. W. Drahushuk, D. Kilcoyne, and M. S. Strano, *Nature Nanotechnol.* **12**, 267 (2017).
- [17] S. Faucher, M. Kuehne, V. B. Koman, N. Northrup, D. Kozawa, Z. Yuan, S. X. Li, Y. Zeng, T. Ichihara, R. P. Misra, N. Aluru, D. Blankschtein, and M. S. Strano, *ACS Nano* **15**, 2778 (2021).
- [18] T. Verhagen, J. Klimes, B. Pacakova, M. Kalbac, and J. Vejpravova, *ACS Nano* **14**, 15587 (2020).
- [19] R. H. Tunuguntla, R. Y. Henley, Y.-C. Yao, T. A. Pham, M. Wanunu, and A. Noy, *Science* **357**, 792 (2017).
- [20] B. Radha, A. Esfandiari, F. Wang, A. Rooney, K. Gopinadhan, A. Keerthi, A. Mishchenko, A. Janardanan, P. Blake, L. Fumagalli *et al.*, *Nature (London)* **538**, 222 (2016).
- [21] N. Wei, X. Peng, and Z. Xu, *ACS Appl. Mater. Interfaces* **6**, 5877 (2014).
- [22] Q. Yuan and Y.-P. Zhao, *J. Am. Chem. Soc.* **131**, 6374 (2009).
- [23] S. Ghosh, A. Sood, and N. Kumar, *Science* **299**, 1042 (2003).
- [24] B. Mukherjee, P. K. Maiti, C. Dasgupta, and A. K. Sood, *J. Chem. Phys.* **126**, 124704 (2007).
- [25] S. Chakraborty, H. Kumar, C. Dasgupta, and P. K. Maiti, *Acc. Chem. Res.* **50**, 2139 (2017).
- [26] B. Mukherjee, P. K. Maiti, C. Dasgupta, and A. K. Sood, *ACS Nano* **2**, 1189 (2008).
- [27] Y. Lin, J. Shiomi, S. Maruyama, and G. Amberg, *Phys. Rev. B* **80**, 045419 (2009).
- [28] W. L. Jorgensen, J. Chandrasekhar, J. D. Madura, R. W. Impey, and M. L. Klein, *J. Chem. Phys.* **79**, 926 (1983).
- [29] S. Plimpton, *J. Comput. Phys.* **117**, 1 (1995).
- [30] J. Wang, R. M. Wolf, J. W. Caldwell, P. A. Kollman, and D. A. Case, *J. Comput. Chem.* **25**, 1157 (2004).
- [31] J. Majumdar, M. Moid, C. Dasgupta, and P. K. Maiti, *J. Phys. Chem. B* **125**, 6670 (2021).
- [32] W. Shinoda, M. Shiga, and M. Mikami, *Phys. Rev. B* **69**, 134103 (2004).
- [33] G. J. Martyna, D. J. Tobias, and M. L. Klein, *J. Chem. Phys.* **101**, 4177 (1994).
- [34] F. Zhu, E. Tajkhorshid, and K. Schulten, *Biophys. J.* **83**, 154 (2002).
- [35] See Supplemental Material at <http://link.aps.org/supplemental/10.1103/PhysRevB.107.165402> for pair correlation function, dipole trajectory, dipole profile during orientational jumps and dwell time for different CNT lengths.
- [36] D. Laage and W. H. Thompson, *J. Chem. Phys.* **136**, 044513 (2012).
- [37] D. Laage, G. Stirnemann, F. Sterpone, and J. T. Hynes, *Acc. Chem. Res.* **45**, 53 (2012).
- [38] J. Köfinger, G. Hummer, and C. Dellago, *Proc. Natl. Acad. Sci. USA* **105**, 13218 (2008).